CEA-CONF-10557

FR 92/1/54

ICF RELATED EXPERIMENTS AT CEL-V.

21 st. ECLIM . WARSAW.
OCTOBER 21-25 ,1991.

Authors:M.Andre, C.Bayer, D.Babonneau, M.Bernard,
JL.Bocher,J.Bruneau, A.Coudeville, J.Coutant,
R.Dautray, A.Decoster, M.Decroisette, D.Desenne,
B.Duborgel, JM.Dufour, JP.Jadaud, D.Juraszek,
JP.Garconnet, PA.Holstein, J.Lachkar,M.Louis-Jacquet,
F.Mucchielli, B.Meyer, JP.LeBreton,J.Ouvry,
D.Schirmann, G.Schurtz, D.Véron, JP.Watteau.

ABSTRACT.

Implosion experiments performed at Centre d'Etudes de Limeil-Valenton in the indirect drive scheme using the two-beams Nd glass laser facility Phebus at the energy level ≈ 6 kJ (blue light) are presented. A final density of compressed DT close to 100 ρo has been obtained. The best irradiance uniformity on the microballoon was evaluated to ≈15% rms; it has been deduced from radiochemistry of the activated silicon atoms in the pusher. Phebus has also been equipped with an optical fibre oscillator, in order to study the effect of a smoothing technique on coupling processes: it appeared that at 0.53 μm, absorption efficiency is increased by ≈15-20%. With the eight beams Octal laser, hydrodynamic instabilities development in accelerated planar targets has been investigated both for direct and indirect drive; the mixing zone which is detected at light-heavy interface does not present visible bubble-and-spike like structures , and is less developed in the indirect configuration.

Atomic physics in laser plasmas is also deeply studied; a particular effort has been made on absorption spectroscopy which is a powerful diagnostic of ionization dynamics in cold and dense plasmas. Experiments have been realized either in multilayered targets, or using rear side x-ray emission of thin gold foils to heat the samples.

In order to reach fuel ignition conditions, much powerful lasers, in the range of megajoule, will be needed. Their design needs further technological developments in order to reduce the capital cost in $ /W. At Limeil, we work mainly on high damage threshold optical coatings, using the sol-gel process, high quality - low cost mirror fabrication, using the replica technics and incoherent laser pulse generation for beam smoothing.

Summary:

Introduction.

X-ray conversion and radiative transfer.

X-ray driven implosions.
- Irradiance uniformity.
- Compression measurements.

Hydrodynamic instabilities.
- Direct drive experiments.
- Indirect drive experiments.

Effect of optical smoothing.

Atomic physics in x-ray driven plasmas.

High power laser technology.

Conclusion.

INTRODUCTION.

The objective of Inertial Confinement Fusion is to dispose of a laboratory facility delivering 100 -1000 MJ in energy, starting from a 10 MJ driver. Four candidates are considered: glass or gas lasers, light or heavy ions beams. The principle of ICF is to compress up to a thousand times the liquid density a small sphere of DT which ignites and burns before being decompressed. High gain (i.e ≈100) can be obtained from a "hot spot" structure, constituted of an ignition spark (areal density > 0.3 g/cm^2, temperature > 5 keV) where α particles are reabsorbed - what generates a self sustained thermonuclear burn wave - surrounded by a large amount of cold compressed fuel (areal density > 3 g/cm^2) [NUCKOLLS et al 1972; COUTANT et al 1987; STORM et al 1988]. An important intermediate step to be attained on this way is to fulfill the ignition conditions of the DT capsule, if possible with small gain. Most of the laboratories involved in this program agree that this goal can be reached with a few megajoule Nd glass laser, the technology of which is the most developped to day.

The physics of implosion - laser-plasma coupling, energy transport, induced hydrodynamics...- has been widely studied in small scale experiments (laser energy in the range 1 - 40 kJ). First results have been obtained in the exploding pusher regime, characterized by a high temperature but a low final density [see for example: STORM et al 1978; YAAKOBI et al 1979; LAUNSPACH et al 1981]. High densities require a so-called ablative regime, with more elaborated target structures and tailored laser pulses; key issues of such a process are well known:

- an irradiation uniformity ≈ 1 %, to preserve the hydrodynamical stability of the implosion;
- a DT compression mode close to an isentrope (a fuel preheat less than a few eV).

Laboratories involved in ICF explore two different approaches to realize the most efficient energy transfer to the target, and get over these difficulties:

- either the "direct drive" scheme, in which the microsphere is irradiated by several laser beams organized in order to insure the best irradiation uniformity [BASOV et al 1980; McGOWAN et al 1983; BAYER et al 1984; McCRORY et al 1990; AZEKI et al 1990; JOHNSON et al 1990];
- or the "indirect drive" scheme, in which the laser radiation is first converted into thermal x rays [NUCKOLLS 1982;YAMANAKA et al 1984; ANDRE et al 1990; MURAKAMI et al 1991].

Significative results obtained on the second way with Phebus are presented in this paper.

X-RAY CONVERSION EFFICIENCY AND RADIATIVE TRANSFER.

Absorption and generation of soft x rays (which constitute the driving energy in implosion experiments) have been widely studied as function of irradiation parameters (laser wavelength, irradiance, pulse duration) and target characteristics (material, thickness) [BABONNEAU et al 1991; JURASZEK et al 1991; GABL et al 1990]. At λ=0.35μm the fractional absorption in thick planar gold targets is greater than 90% for irradiances up to 10^{15}W/cm^2, and an x-ray conversion efficiency up to 60% has been measured with Phebus for irradiances $\approx 10^{14}$ W/cm^2 in 1.3 nsec pulses (**fig.1**). Most of the energy is emitted in the range hv$\leq$ 1 keV with a radiation lobe intermediate between black-body and isotropic ones.

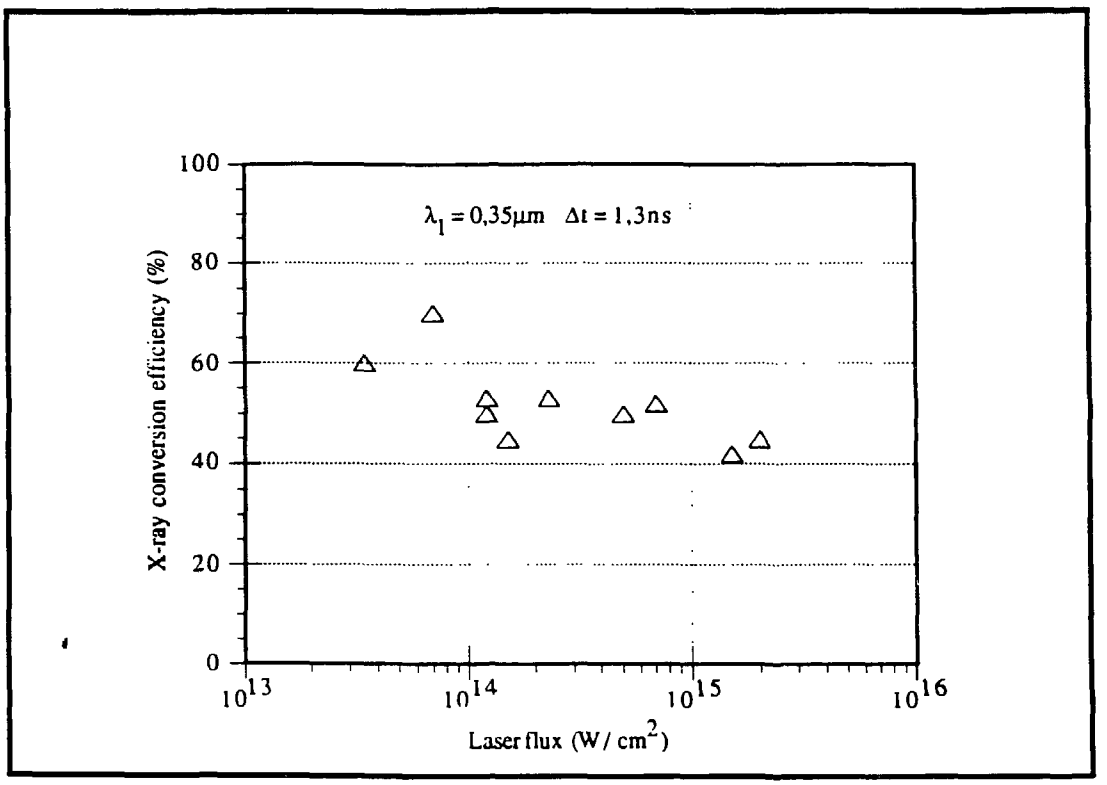

Fig. 1: X-ray conversion efficiency in laser irradiated planar gold targets.

Several aspects of radiative transfer, among which soft x-ray re-emission, have to be analyzed to get a satisfactory understanding of radiation confinement in cavities. Albedo experiments have been performed in planar geometry with Phebus facility [JURASZEK et al 1990].

The structure of the target is shown **fig. 2**; it has been defined in order to ensure a high signal/noise ratio. The x-ray source is created at the bottom of a box-shaped gold target, edges of which prevent primary x rays to shade the re-emission. The gold re-emitter is ring shaped to maximize the re-emission surface at a given incidence; the x-ray irradiance on it has been evaluated to = $5.10^{12}W/cm^2$.Time resolved spectral analysis of the re-emission was performed

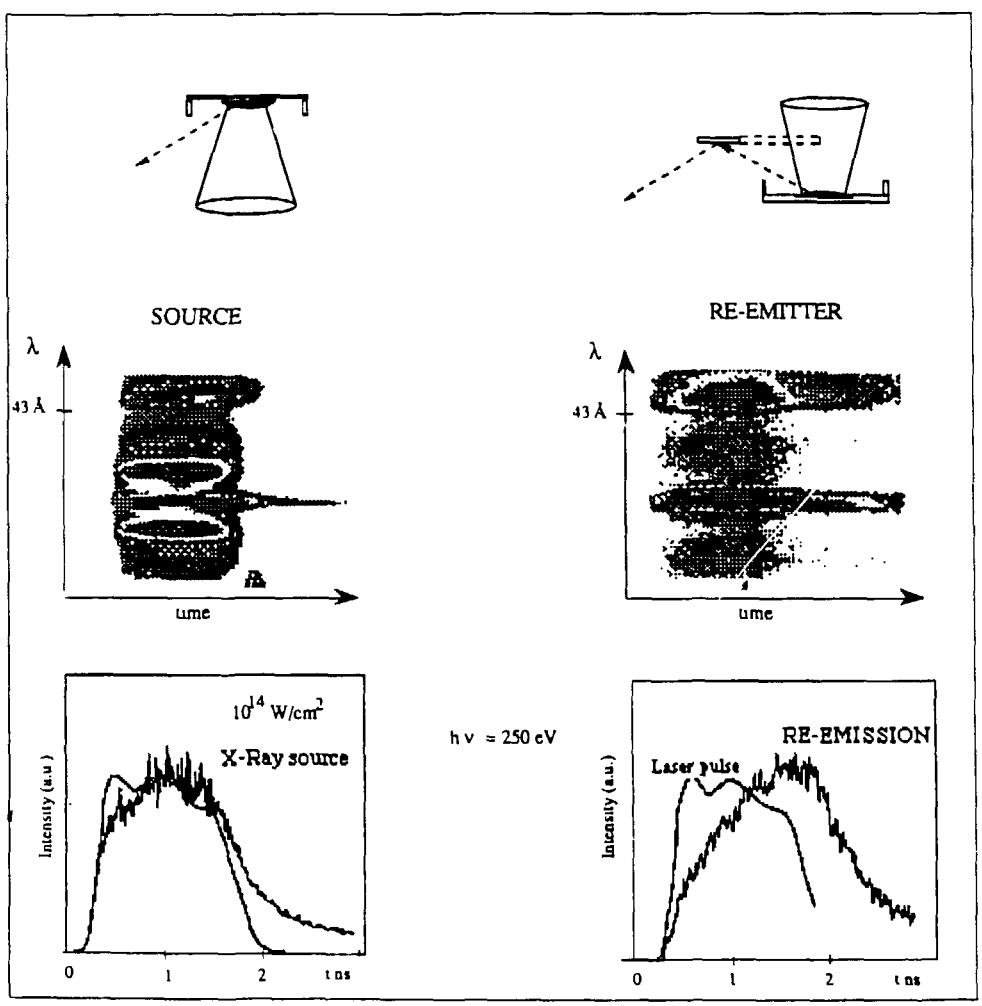

Fig 2: Albedo experiment. Spectral analysis of primary and re-emitted x rays.

with a streaked soft x-ray broad band spectrometer constituted of a transmission grating fit for use in the range 40 eV-1 keV, associated with a streak camera [ANDRE et al 1988]; time and spectral resolutions were respectively: 40 ps and $10<\lambda/\Delta\lambda<100$. A qualitative comparison was made with the source emission. **Fig. 2** displays the recorded spectra; The strong variation near 43Å is due to the K-edge absorption of a plastic filter. A significant difference in the temporal evolution between primary and re-emitted x rays, for example at $h\nu \approx 250$ eV, is clearly evidenced.

X-RAY DRIVEN IMPLOSIONS.

The indirect drive scheme (or x-ray driven), involves a high Z cavity (or "hohlraum") enclosing the proper fusion target. Laser beams, through small dimension holes, irradiate the inner side of the wall. Focusing conditions are defined in order to optimize the conversion into soft x rays; confinement concludes in the generation of a nearly Planckian x radiation [TSAKIRIS et al 1990](equivalent black-body radiation temperature ≈ 200 eV) which ablates and implodes the pellet.

The efficiency of energy transfer to the microballoon is smaller than in the direct drive case, and parasitic effects due to the filling up of the cavity by expanding plasma can affect the implosion [POLLAINE et al 1991]. However, embedding the pellet in a black-body radiation insures a high irradiance uniformity without drastic constraint on laser beams quality; besides, x-ray driven ablation is propitious to lower the development of hydrodynamical instabilities [KILKENNY 1988].

Experiments at CEL-V have been conducted both with Octal (1.5 TW at λ=1.06 μm, and 0.4 TW at 0.35 μm), and Phebus (5 kJ in 1.3 ns at λ=0.35 μm) since 1986, using plastic coated microballoons filled with DT gas. The **fig. 3** shows the structure of a target designed for Octal. The hohlraum is constituted of two gold hemispheres; the eight beams (individual f number= f/6) arranged in two clusters (effective f-number f/1) enter the cavity through two polar apertures; the dashed curves schematize the irradiation areas. An equatorial slit allows to observe the microballoon implosion.

Numerous diagnostics have been developed for experiments with Phebus to characterize the target performances. Space and time resolved x-ray devices allow to study the hydrodynamics: compression time, stagnation of the pusher, and symmetry of implosion. The 14 MeV neutron yield is measured

by lead and copper activation systems; the burn time is determined with an accuracy = 200 ps, using a plastic scintillator coupled with a microchannel-plate photomultiplier; the DT temperature is deduced from neutron time of flight; at last the target compression is determined by measuring the areal density of the pusher (density-thickness product, $\rho.\Delta R$) at time of maximum neutron yield, by neutron activation. The method has already been used in several laboratories [CAMPBELL et al 1980; AZECHI et al 1990]: silicon atoms in the pusher are activated via the $^{28}Si(n,p)^{28}Al$ reaction; ^{28}Al are counted by $\beta^{-}\gamma$ coincidence technique. The fraction of collected debris is deduced from a radioactive tracer contained in the pusher; actually the tracer is ^{24}Na, formed via the reaction $^{23}Na(n,\gamma)^{24}Na$ by exposing the target to thermal neutrons in a nuclear reactor. The number of activated Al atoms N* is related to the neutron yield N and to the pusher areal density at burn time by: $N^* = k.N.(\rho\Delta R)$, where k includes the fractional abundance of Si atoms in the pusher, and the cross section of neutron induced reaction. The compressed fuel density is deduced assuming mass conservation, uniform distribution of density and isobaricity throughout the fuel and pusher regions.

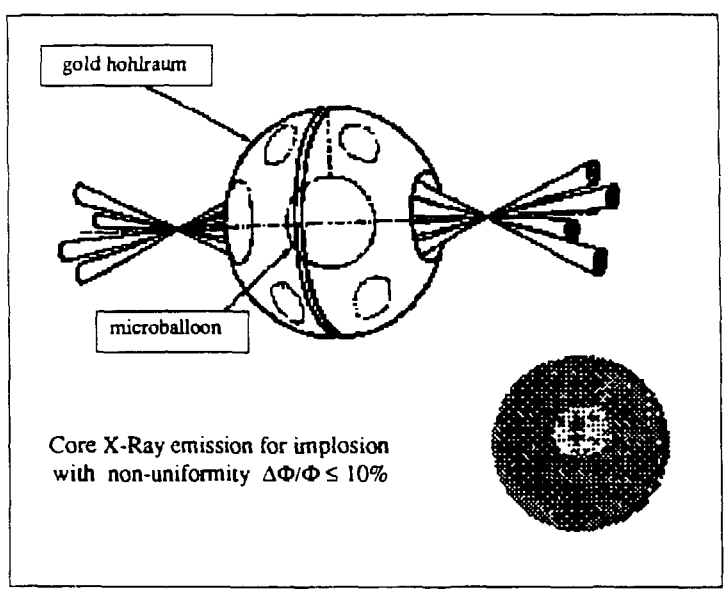

Fig. 3: Hohlraum target structure for implosion experiments with the eight beams laser facility Octal. Sphericity of the core at stagnation is evaluated from time integrated x-ray pinhole picture ($h\nu$>1keV).

Irradiance uniformity.

In exploding pusher implosions, the symmetry of compressed core was evaluated from the shape of time integrated x-ray pinhole pictures recorded in the photon range $h\nu > 1$ keV. It was proved that the implosion symmetry could be controlled by the hohlraum structure. Several pictures, obtained for different cavity geometries tested on Phebus, are presented **fig. 4**. In these experiments the x-ray emission comes from the compressed pusher at stagnation time; the spatial distribution of zones on which maxima of emission appear located is schematized below. Symmetry increases from left to right. The two last cases correspond to ellipsoid shaped cores (a and b being the ellipse axis); in the last picture, the core emission has been partly occulted by the cavity, but appears to be nearly spherical; in such a case, a convergence ratio (ratio of the pusher initial ratio to the final one) can be defined. The higher values of convergence ratio obtained in ablative experiments range around 15 ± 5, in a good agreement with numerical simulations.

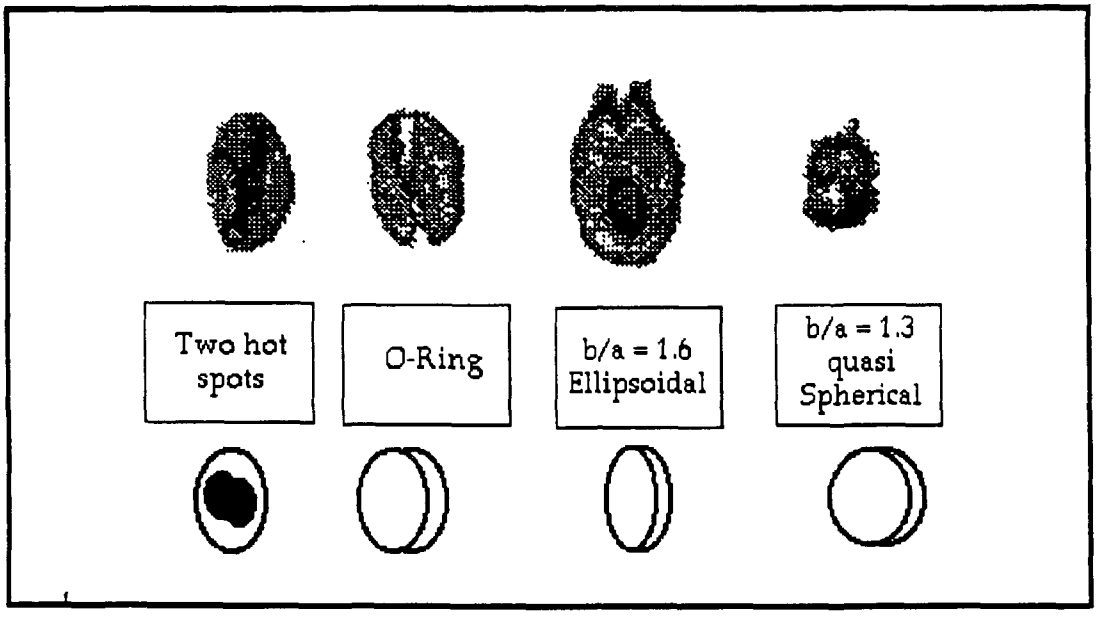

Fig. 4: Implosion experiments with Phebus. Effect of hohlraum geometry on x-ray core emission.

The spatial distribution of core emission (deviation from sphericity) can be related through analytical models and numerical simulations to the on-target irradiance. The fourth case in **fig.4** corresponds to a non uniformity

$\Delta\Phi/\Phi < 15\%$ (RMS). Similar x-ray picture recorded with Octal, presented fig 3, shows that a better uniformity has been obtained with eight beams ($\Delta\Phi/\Phi <$ 10% RMS).

Numerical simulations are performed with the FCI2 code, characteristics of which have been already described [MUCCHIELLI et al 1988]; it is a two dimensional lagrangian code with limited heat flux conduction, multigroup radiation diffusion, and non LTE package for gold; post processors can be coupled to simulate the diagnostics. As an example, a comparison between experimental and numerical x-ray pictures is presented **fig. 5** ; agreement appears quite good.

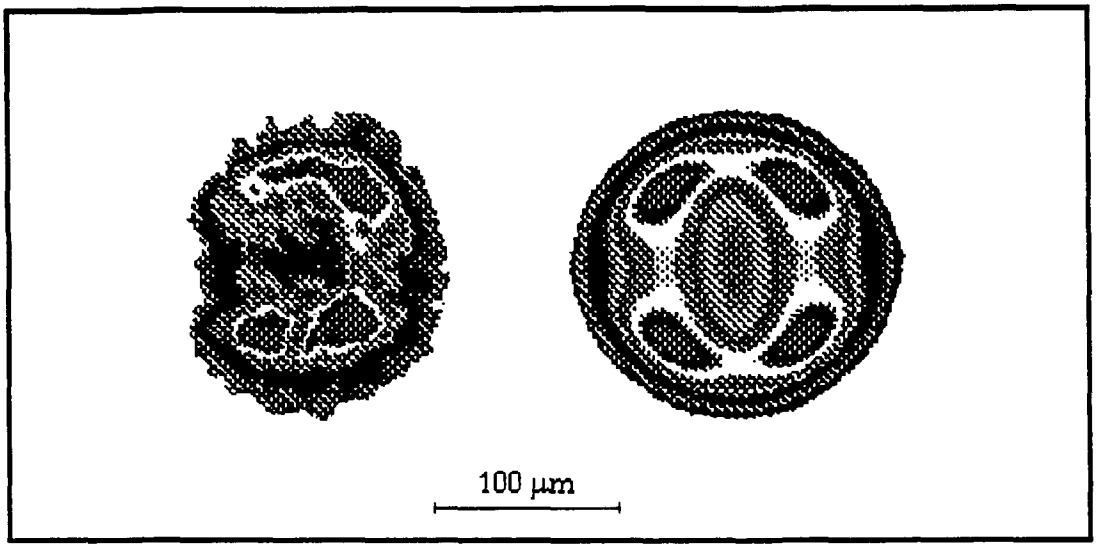

Fig. 5: Comparison between experimental time integrated x-ray pinhole picture ($h\nu > 1$ keV), and FCI2 numerical simulation. (Same space scale and color levels).

Compression measurements.

A series of experiments have been conducted with Phebus, varying the initial pusher thickness in order to progress towards high fuel densities.

The variation of areal density of the pusher at burn time, normalized to the initial value $(\rho.\Delta R)^f/(\rho.\Delta R)^i$ is plotted **fig.6.** It appears to increase with the initial pusher thickness (by roughly one order of magnitude over the explored region); the highest areal density ratio is seen to be about 100. Jointly, the neutron yield decreases from $\approx 10^9$ to $\approx 10^7$ neutrons.

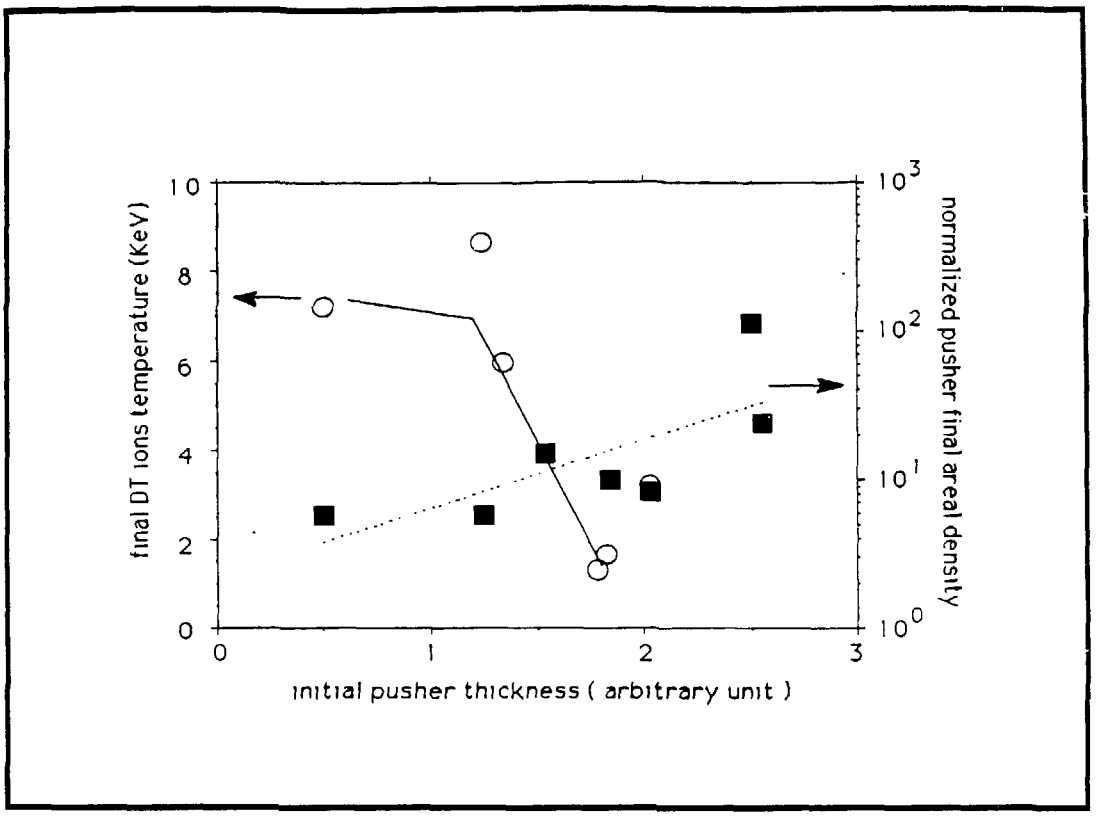

Fig.6: Variations of the final DT temperature and normalized pusher areal density, versus the initial pusher thickness.

All these features are coherent with an evolution from high adiabat implosion (low densities, high temperatures) towards more ablative ones. The density of compressed core, deduced from the values of final pusher areal densities, is plotted versus the neutron yield **fig.7**. Results are close to those presented by other laboratories for similar experiments (x-ray driven implosions, plastic coated glass microballoons filled with DT gas) [ZE et al 1985; YAMANAKA et al 1986; STORM et al 1988]. This figure shows that a compressed DT density close to $\approx 100\rho_0$ (ρ_0 = liquid DT density) has been obtained.

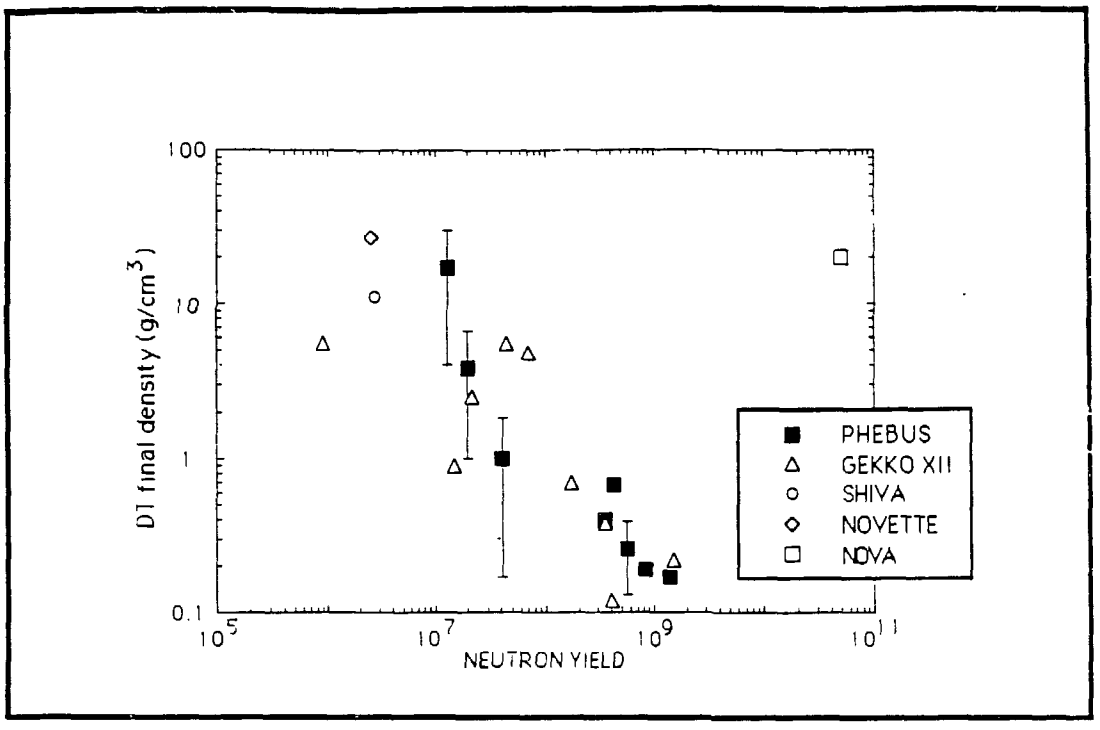

Fig. 7: Phebus implosion experiments. Comparison of performances with other laboratories.

The neutron yields obtained in these experiments have been compared with one dimensional predictions; the evolution of ratio versus the calculated convergence ratio is presented **fig.8**. A correct agreement is obtained for exploding pusher type implosions (lower convergence ratio), while two orders of magnitude in difference are observed for higher convergence ratios.

Reduction of neutron yield below 1D simulation yield has already been observed [McCRORY et al 1990; KILKENNY et al 1988]. The primary limitation of an ablative implosion is the distance the pusher can travel before the structure is broken up; non uniformities of drive flux, already mentioned, may be obviously the first origin of discrepancy. Even if the irradiance uniformity is good enough to maintain a near spherical implosion up to high convergence ratios, the development of hydrodynamic instabilities can deeply lower the performances. Two stages are instable (according to Rayleigh-Taylor for example): during the acceleration at the ablation front, and during the slowing down at the pusher interface. These instabilities can lead to the penetration of pusher spikes into the fuel, and finally to a mixing, a small amount of which strongly degrades the neutron yield.

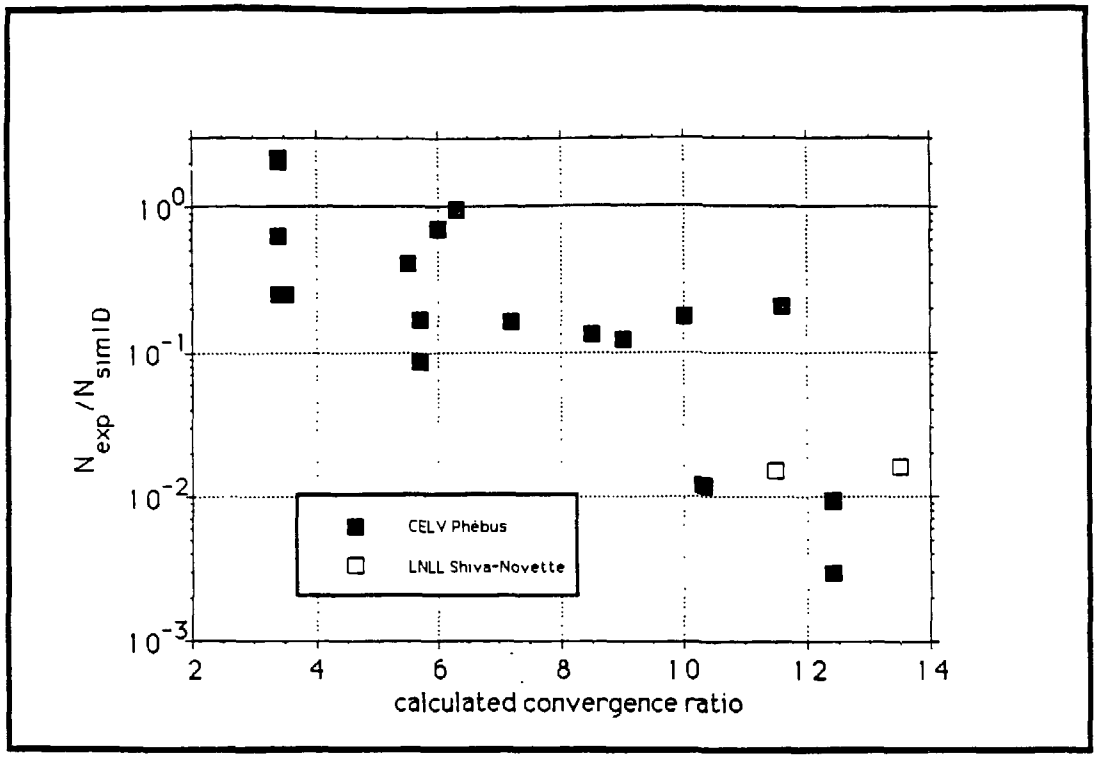

Fig. 8: Experimental neutron yield normalized to 1D simulations.

HYDRODYNAMIC INSTABILITIES.

Owing to the drastic consequence they can have on implosion performances, these processes are deeply investigated [KILKENNY 1990; MIKAELIAN 1990]. At CEL-V, we performed experiments on directly or indirectly driven planar targets, in which mixing is expected to occur [HOLSTEIN et al 1988](**fig. 9**).

The principle is to accelerate a layered target involving a light-heavy interface. As the shock breaks through, the situation of a light fluid pushing a heavy one is similar to the slowing down of the pusher by the fuel, and mixing can develop. After some delay, the mix is detected by a spectroscopic method: the rear side of the accelerated target is heated by a probe beam, set to ablate the heavy material over a depth inferior to the initial thickness; the eventual detection of x-ray lines specific of light material is the signature of a mixing.

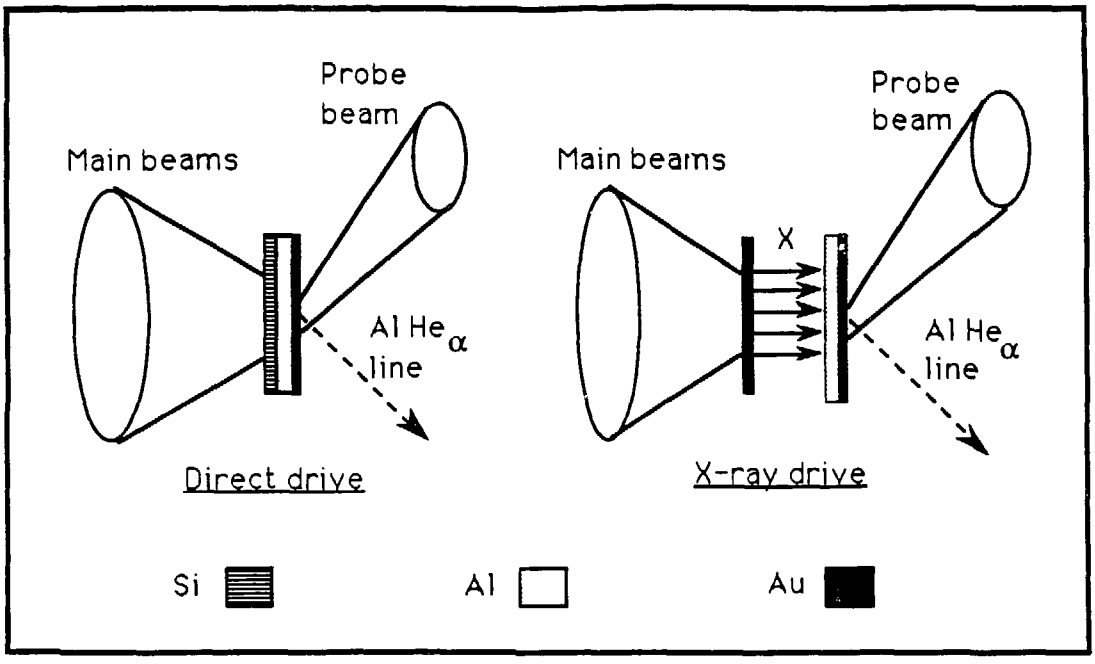

Fig. 9: Principle of R.T instabilities study in layered targets .

Aluminium and gold have been chosen to constitute the target, and relevant diagnostic was the temporal evolution and the energy of Al Heα line emission. Direct drive was realized at 0.35 μm with optically smoothed beams (RPP); for indirect drive, the source was the soft x-ray emission from the rear side of a laser irradiated thin gold foil.

In the case of direct drive, a third silicon layer was added at the front, to keep the aluminium from direct heating, which would have produce a spurious Al emission; the resultant Si-Al interface has no major effect on the hydrodynamics as it is stable according to Rayleigh-Taylor, owing to its faint density jump.

A most important feature of the experiment was to check the method on a "null-mix" experiment, using a stable target obtained by replacing the gold layer by a silicon one.

The variation of the Al Heα line energy versus the laser irradiance is presented **fig.10**, for different unstable targets. The probing delay was set to 1 (direct drive) to 2ns (indirect) after the main irradiation; at that time, the shock has already broken through the Al/Au interface and the whole target has moved over a distance depending on its mass and on the irradiance. That recoil was either measured from side-on x-ray shadowgraphy (for

displacements greater than the spatial resolution),or deduced from numerical simulations.

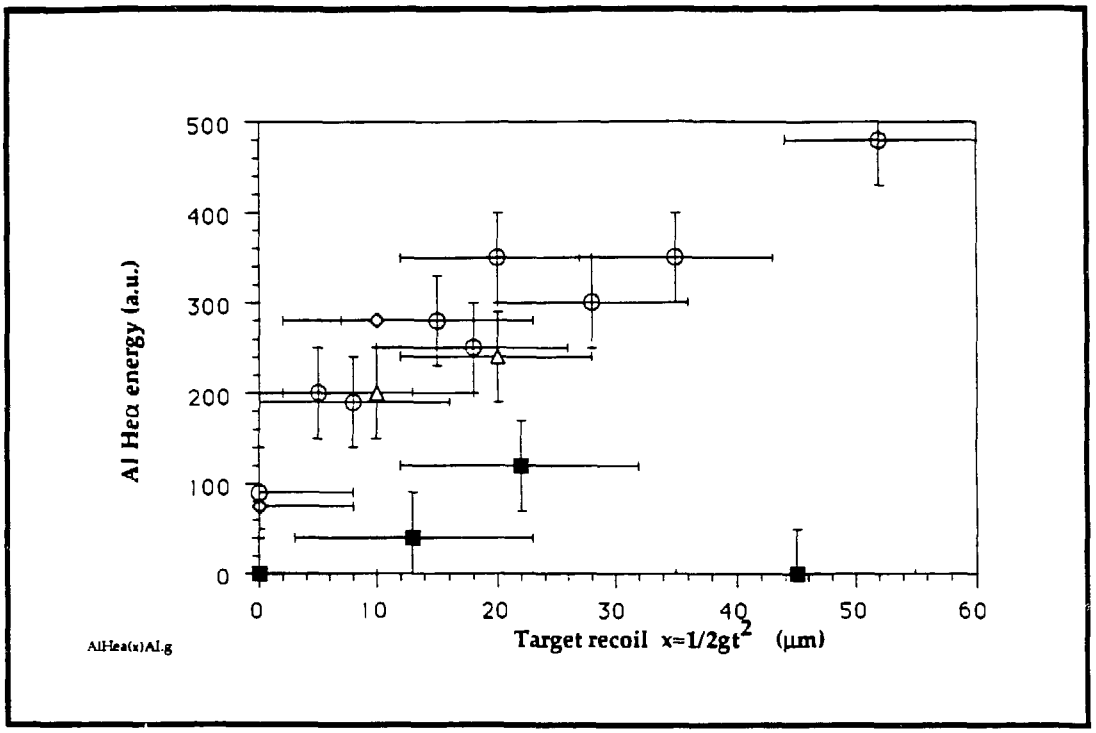

Fig.10: Mix evolution with laser irradiance and target recoil, for direct (open points) and indirect (black squares) driven targets.

For direct drive experiments the variation of Al Heα line intensity is seen to increase with recoil. Indeed, the mixing is expected to be more important for greater accelerations. It is noticeable, however, that it is significant even for small recoils, and that the rate of increase is rather moderate. In the indirect drive case the mixing appears significantly smaller.

The temporal profiles of Al Heα line shows an important feature of these experiments: the aluminium emission starts simultaneously with the gold one which itself follows the temporal profile of the probe beam; that reveals an early mixing, with a far penetration of aluminium into gold even for low driving irradiances. It is fully different from what is observed on stable targets: in that case, Al Heα line emission appears after the beginning of the laser probe beam, with a time delay in agreement with the propagation time calculated for the thermal wave in the silicon layer ; that means the probe beam does not induce Rayleigh-Taylor type instabilities at the rear side ablation

front, what validates the diagnostic.

X-ray face-on shadowgraphy observations performed on the same target configurations [HOLSTEIN et al 1991] did not evidenced bubble-and-spike structures, within the spatial resolution (≈15 μm). Mixing may be thus considered as homogeneous .

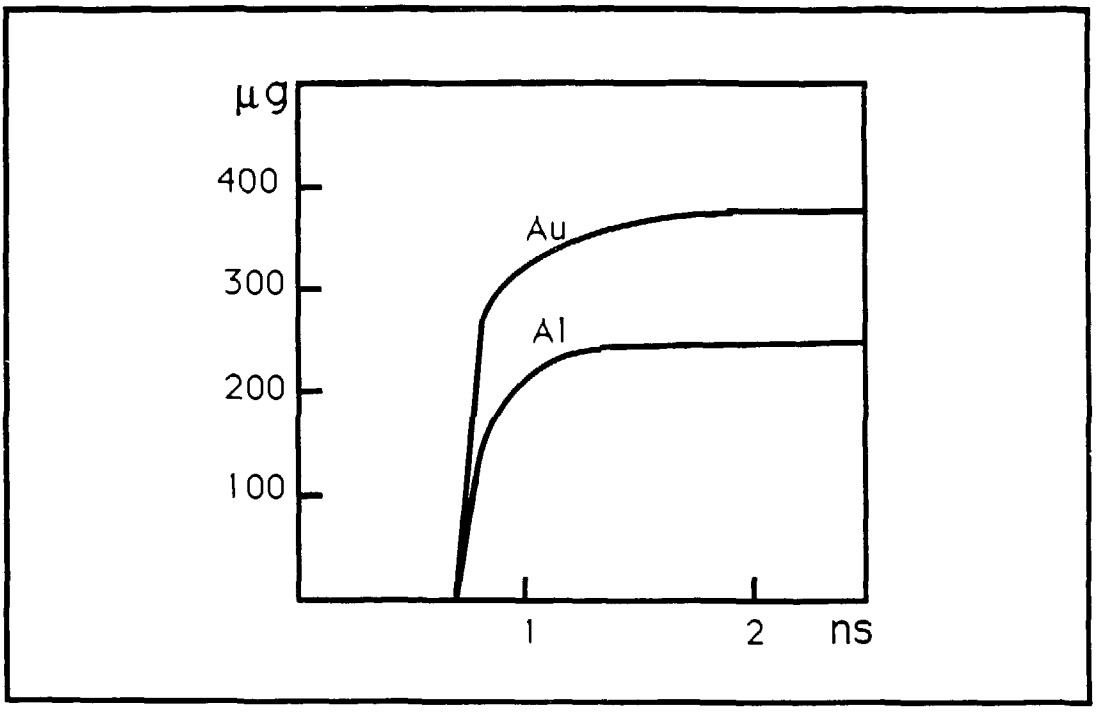

Fig. 11: "k-ε" simulation of direct drive unstable targets; temporal evolution of Au and Al undergoing mixing;
Initial masses: Au,495 μg; Al,450μg.

These results raise several important questions:

- What kind of instabilities are generated at the Al-Au interface? Rayleigh-Taylor instabilities can be a priori invoked. They refer to perturbations at the interface between two fluids undergoing acceleration; successive phases of development are linear regime (exponential growth of perturbation amplitude), nonlinear regime (bubble-and-spike structures), and developped turbulence. The apparent homogeneity and the small increase of mixing versus target recoil (or acceleration) incited us to simulate the experiment with a statistical model of developed turbulence [GAUTHIER et al

1990] coupled with the FCI code. The temporal variation of Al and Au materials undergoing mixing for a direct drive case is presented **fig.11**; the echelon type evolution is compatible with the experimental observations. However, the possibility of a Richtmyer-Meshkov type instability, which occurs when a shock crosses the interface, cannot be rejected. Further experiment will have to check this point.

- What is the reason for a smaller mixing in the indirect drive case?

Several answers can be proposed. Obviously, x-ray drive offers a smoothness of irradiation much better than laser one, even with random phase plate. However, ablation and density gradients are known to reduce the growth rate of the Rayleigh-Taylor instability; these stabilization mechanisms seems to be more effective for shorter wavelengths, and thus a fortiori for x rays [KILKENNY et al 1988]. Both effects may operate in our experiment.

EFFECT OF OPTICAL SMOOTHING.

High level of irradiance uniformity is a key issue in ICF research. Smooth intensity pattern is important even in the indirect scheme, as hot spots can set off various parametric instabilities such as stimulated Brillouin scattering, stimulated Raman scattering, filamentation, which in turn generate hot electrons and preheat the fuel.

An optical smoothing technique based on a fiber laser oscillator has been developed at CEL-V [VERON et al 1988]. After being tested on the single beam facility P102, this technique has been implemented on Phebus.

The output beam of an oscillator, made with a silicate and a phosphate glass rods placed in serie in the same cavity, is injected into a 50m long multimode optical fiber. The bandwidth of the 1 ns duration pulse is adjustable from 1 to 2 nm. The dispersive effect of the fiber transfers the temporal incoherence into spatial incoherence. Then, hundred of different interference patterns are successively superimposed at the fiber output during the whole time duration of the pulse, and smoothing results from the time averaged energy distribution at the fiber output [VERON et al 1988].

Indeed, direct optical measurements of the energy distribution in the focal spot as well as target x-ray images show that the irradiance uniformity is greatly improved with respect to the usual standard beam system.

However, the maximum energy obtainable at the 1.06 μm wavelength and with a pulse duration of 1.3 ns is limited at 5.1 kJ, whatever the amplifier

chain input energy is, compared to the 9kJ when using the unsmoothed configuration.The near field pattern does not show any strong self-focusing effect, but scraping of the top of the temporal output pulse is evidenced and limits the fluence to about 2.4 GW/cm^2. A tentative explanation is that the hot spots of the instantaneous speckle pattern generate non linear effects in the amplifying medium. It is suggested that a two-photon absorption like phenomenon [PENZKOFER et al 1972] combined with simultaneous Kerr effect, may be responsible for the observed limitation. Further experimental and theoretical investigations are in progress to clarify this important point.

The efficiency of the frequency doubling using the smoothing configuration decreases with respect to that obtained with the standard oscillator, above a fluence of 1.4 GW/cm^2, at which scraping begins to appear.

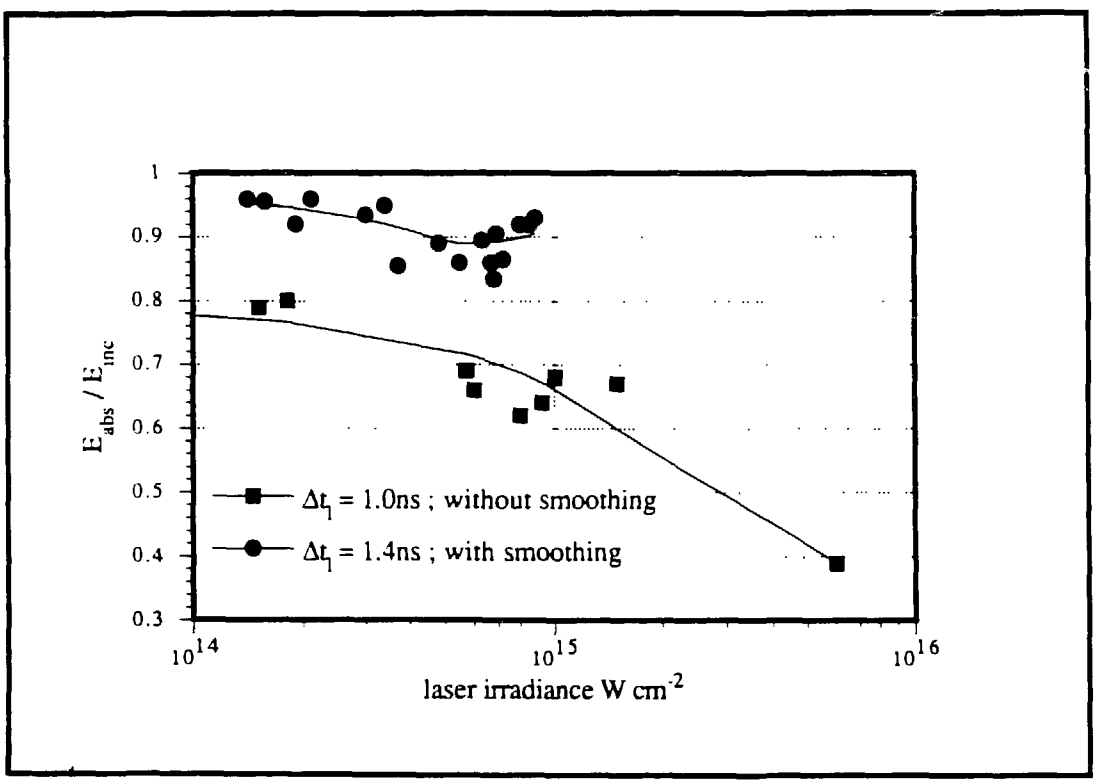

Fig. 13: Effect of optical smoothing on laser light absorption efficiency at λ = 0.53 μm.

A series of experiment have been conducted to study the effect of beam smoothing on interaction physics. Other laboratories are involved in this

subject and the results we present are complementary to recent publications [ANDRE et al 1988;BOSCH et al 1991; KANIA et al 1991].

Experiments were performed at 0.53 μm (pulse duration: 1.4 ns) on planar gold targets, in the irradiance range 10^{14} - 10^{15} W/cm^2. Comparison was made with previous ones realized at the same wavelength with a standard oscillator. Typical results on absorption and x-ray conversion efficiencies are presented **fig.13 & 14**. A significant increase of laser light absorption ≈ 20 % was observed,arising from a significant reduction of the backscattered light (factor ≈10 for a f:6 aperture lens). On the other hand, the x-ray conversion efficiency is nearly unchanged, as well as the global features of the x-ray spectrum; however a small reduction of the hard x-ray level is noticed (for example a factor ≈ 3 at hν = 20 keV).

Whether the increase of absorption is due to the smoothness of irradiation, or to the increased spectral width of laser light is not yet understood.

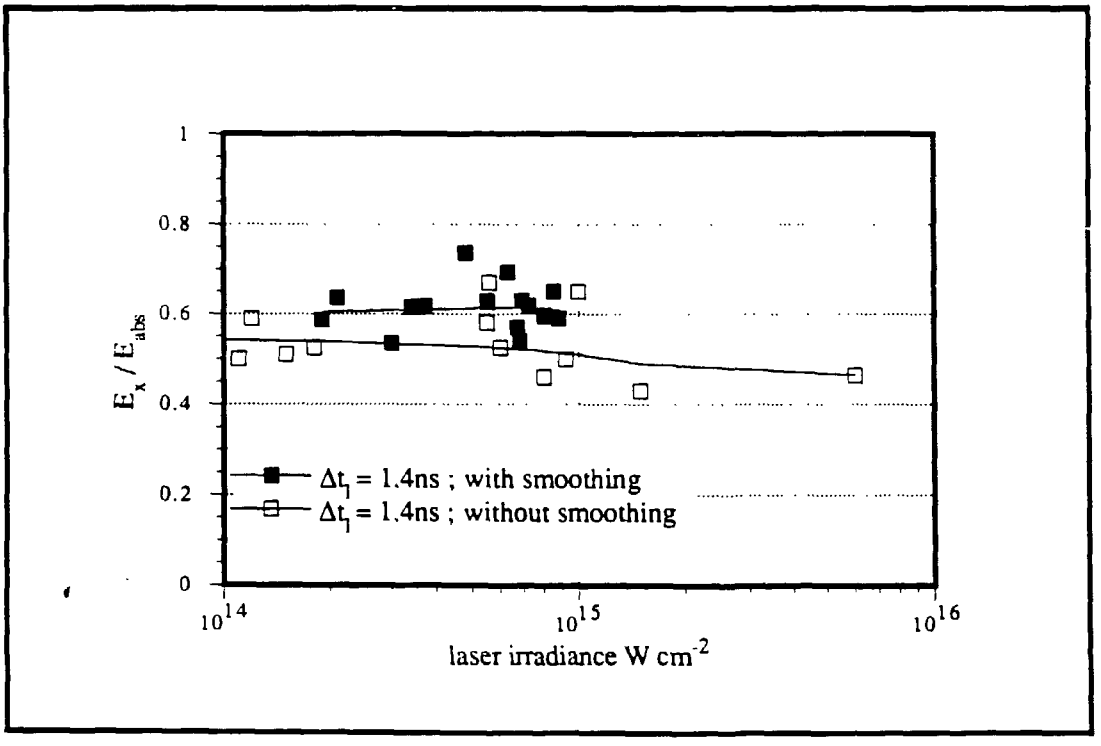

Fig. 14: Effect of optical smoothing on x-ray conversion efficiency at λ = 0.53 μm.

ATOMIC PHYSICS IN X-RAY DRIVEN PLASMAS.

For indirect drive capsule design, the temporal evolution of electron temperature and density of x-ray created plasmas has obviously to be satisfactorily described. x-ray absorption spectroscopy has been proved to be a very powerful diagnostic tool for such plasmas .

In recent experiments performed on Octal in collaboration with CNRS , we evidenced for the first time the L-shell absorption. In the first series [BRUNEAU et al 1990], the target consisted in a three-layer foil; the first layer, made of praseodymium, created a radiative wave which, after crossing a silicon spacer, heated the material to be probed (germanium layer); the praseodymium emission was also used as the x-ray source for absorption spectroscopy. In the second series [BRUNEAU et al 1991] the target structure was improved, with separated heating and probing functions : the sample was heated by the rear side x-ray emission from laser irradiated thin gold foils, and probed by absorption of the radiation emitted from a praseodymium backlighter produced by an auxiliary time-delayed laser beam.

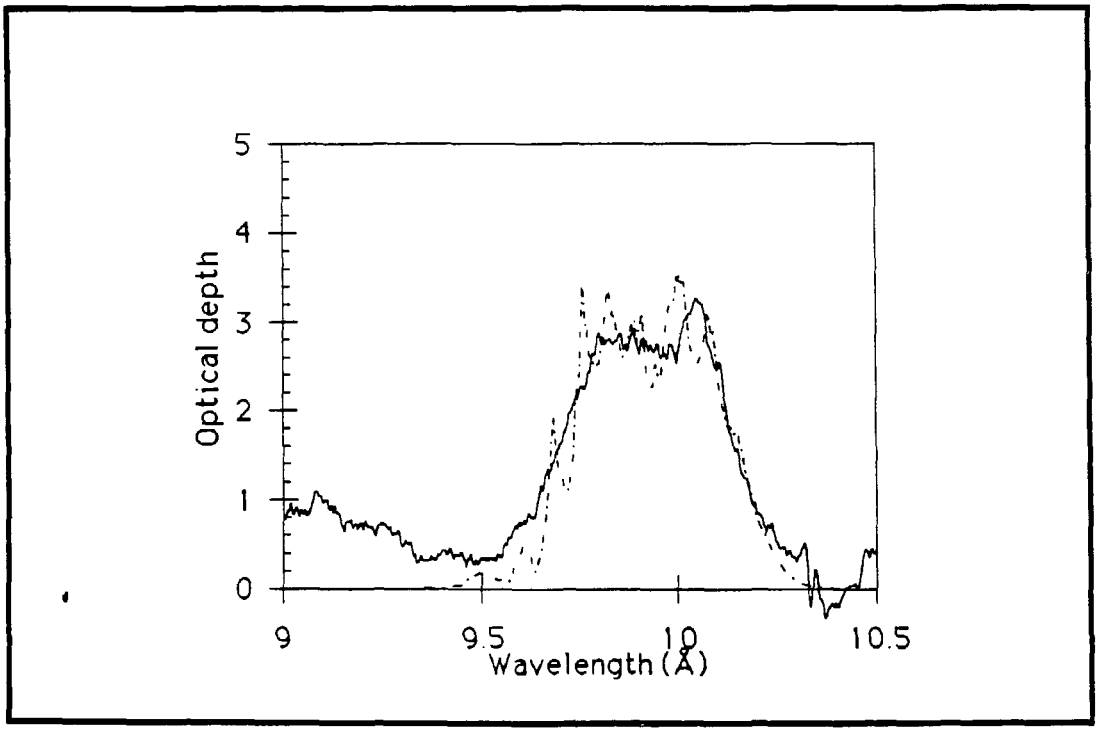

Fig. 15: Optical depth of germanium as a function of wavelength; solid line:experimental spectrum; dashed line: calculated spectrum.

In both cases, the L-shell absorption structure has been characterized, and recorded versus time . Results were compared to absorption spectra calculated with a detailed atomic physics code used as a postprocessor to hydrocode simulations. Owing to the good agreement obtained (**fig.15**), the time evolution of the ionization degree and the electron temperature was inferred.

HIGH POWER LASER TECHNOLOGY

The evolution towards higher energy and power on target requires improvements in laser structures and in components design [ANDRE et al 1991]. In order to improve the performances of our existing facility Phebus and to prepare future projects, we have decided to concentrate our efforts mainly on the development of high damage level mirrors associating the fabrication of low cost substrats made by the replication technique (**fig.16**) with optical coatings deposited at room temperature by the sol-gel process [FLOCH et al 1990].

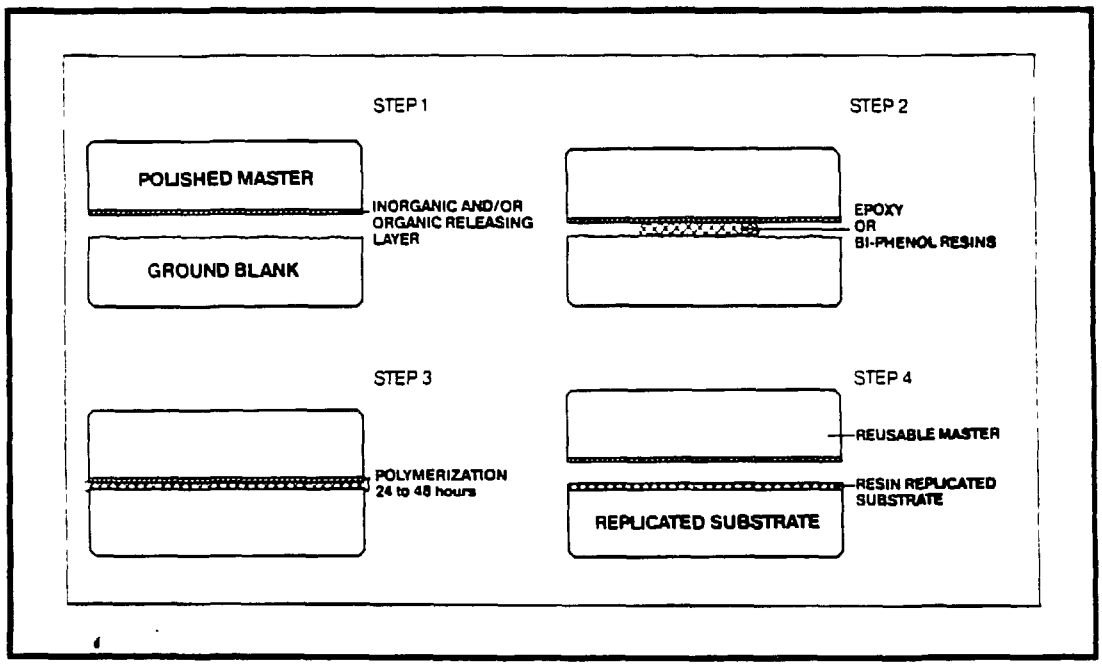

Fig. 16: Principle of replication process.

Sol-gel is already used on high power lasers as anti-reflective coating on silica lenses and KDP crystals (**fig.17**) In order to be able to produce mirrors, several high index materials such as ZrO2, HfO2, and Al2O3-H2O have been developed. Using the spin coating deposition technique, 20 cm diameter

mirrors have been built and have shown damage thresholds as high as 25 J/cm^2 at 1053 nm and for a 3 ns pulse duration. Our goal is to be able to coat circular mirrors up to 45 cm in diameter or rectangular mirrors of approximately 30 by 45 cm.

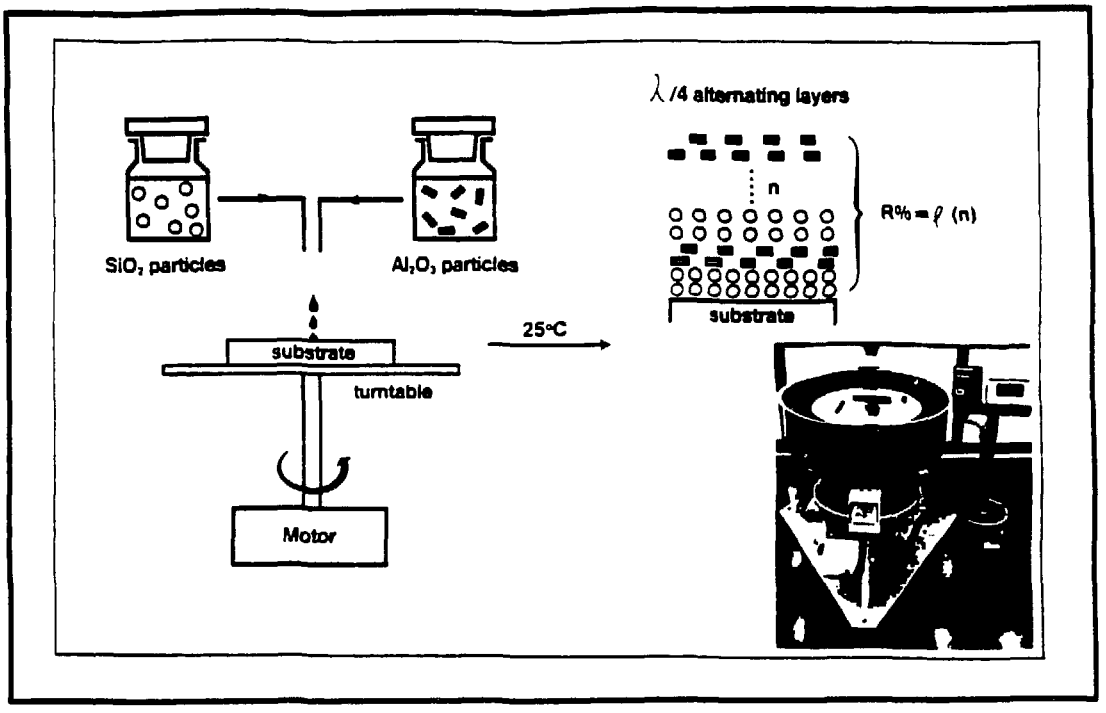

Fig. 17: Schematic description of sol-gel process.

Besides this main activity, we have developed with the European company HAEFELY a compact capacitor able to store 5000 J/l.A prototype , 50 kJ-200μF-20 kV already sustained successfully 10000 discharges. Industrial projection indicates that for important series, the cost could go down to about 0.1$/J and that compacity as high as 1000J/l is possible.

Finally, we are collaborating with the LLNL in the USA on multisegments amplifiers, Pockell's cells development and testing, and design of target chambers for Megajoule laser facility [RABEAU et al 1991].

CONCLUSION

Even if there is to-day no official decision to build in a near future a MJ laser facility with the goal of reaching ignition conditions in the indirect drive scheme, our program is dedicated to the studies of physical and technical main problems to be solved for that purpose.

REFERENCES.

ANDRE, M. et al 1988, Laser Interaction and related plasma phenomena -P.P- 8,503

ANDRE, M. et al 1990, IAEA 13 th Int. Conf. on Plasma physics and controlled Nuclear Fusion; Washington DC,USA.

ANDRE, M. et al 1991, IAEA 14 th Int. Conf. on Plasma physics and controlled Nuclear Fusion; Osaka, Japon.

AZECHI, H. et al 1990, 20th ECLIM Schliersee FRG.

BABONNEAU, D. et al 1991,Laser Part Beams 9,527.

BASOV, NG. et al 1980,Sov Phys JETP 51,212.

BAYER, C. et al 1984, Nucl Fus 24, 573.

BOSCH, RA. et al 1991,Phys Rev 43,953

BRUNEAU, J. et al 1990, PRL 65,1435.

BRUNEAU, J. et al 1991,Phys Rev 44,832.

CAMPBELL, EM. 1980,Appl Phys Lett 36,965.

CAMPBELL, EM. 1991, Laser Part. Beams 9, 209.

COUTANT, J. et al, 1987, Entropie 133,73.

FLOCH ,H. et al 1990, 22th Boulder Dammage Symposium.

GABL,EF. et al 1990,Phys Fluids B2 10,2437.

GAUTHIER, S., BONNET, M 1990, Phys Fluids 9,

HOLSTEIN, PA et al1991 3rd International Workshop on the Physics of compressible turbulent mixing; Royaumont-France.(See also GALMICHE, D. et al 1991,id. MUCCHIELLI, F. 1991,id.)

HOLSTEIN, PA. et al 1988,C.R.Acad Sci Paris 307,211.

JOHNSON, RR. et al 1990, Phys Rev 41,1058.

JURASZEK, et al 1990, 20th ECLIM Schliersee FRG.

JURASZEK, et al 1991, J APPL Phys 70,1980.

KANIA, DR. et al 1991,Phy Fluids 6,1496.

KILKENNY, JD. 1990, Phys Fluids §,1400.

KILKENNY, JD. 1998, IAEA 12 th Int. Conf. on Plasma physics and controlled Nuclear Fusion; Nice France.

LAUNSPACH, J. et al 1981,Nucl Fus 21,100.

MacGOWAN, BJ. et al 1983, Opt Com. 48, 256.

McCRORY, RL. et al 1990, IAEA 13 th Int. Conf. on Plasma physics and controlled Nuclear Fusion; Washington DC,USA.

MIKAELIAN, OK. 1990, Phys Rev 42,3400.

MUCCHIELLI, F et al 1988, IAEA 12 th Int. Conf. on Plasma physics and controlled Nuclear Fusion; Nice France.

MURAKAMI, M. et al 1991, Nucl Fus 31,1315.

NUCKOLLS, JH. 1982, Phys. To-Day 35,9,24.

NUCKOLLS, JH.et al 1972, Nature 239,139.

PENZKOFER, A et al 1972, Appl. Phys. Lett. 21,9.

POLLAINE ,SM. 1991,UCRL 104425.

RABEAU, M. et al 1991, 14th IEEE/NPSS Symposium on Fusion Energy, San Diego Ca, USA.

STORM, EK.et al 1978,PRL 40,1570.

STORM, EK. et al, 1988, UCRL 99427.

TSAKIRIS, GD. 1990, Phys Rev 42,6188.

VERON, D. et al 1988, Opt Com. 65,42.

YAAKOBI, B. et al 1979,Phys Rev 19,1247.

YAMANAKA, C. 1986, Laser Interaction and related plasma phenomena -P.P- 7,395.

YAMANAKA, C. et al 1984, IAEA 10 th Int. Conf. on Plasma physics and controlled Nuclear Fusion; London UK.

ZE, F. et al 1985, Comments Plasma Phys. Controlled Fusion 10,33.